

RESEARCH ARTICLE

The Application of Multiresolution Analysis Wavelet Decomposition of Vibration Signals in the Condition Monitoring of Car Suspension

T. Nowakowski^{1*}, G.M. Szymański¹, M. Jóska², R. Mańczak², and D. Mokrzan¹

¹Institute of Transport, Poznan University of Technology, Poznan 60-965, Poland

²Institute of Machines and Motor Vehicles, Poznan University of Technology, Poznan 60-965, Poland

ABSTRACT - The article addresses the issue of increasing the diagnostic capabilities of the car's suspension in the EUSAMA test. A new, quantitative approach was proposed to enable the assessment of the degree of wear and clearance of the lower suspension mount. An active diagnostic experiment was performed to model the clearance in the lower suspension mounting. During the research, bolts with different diameters were used. In the signal analysis, wavelet decomposition into 12 levels was performed using the Db4 wavelet. The resonance area of the system was extracted from an approximate signal, which contained 43.5% of the relative energy. From these signals, a number of point vibration measures were calculated. Finally, the maximum value was selected due to its sensitivity to the condition, which was 48% more than the original EUSAMA results. Based on the selected diagnostic parameter, a clearance model allowing for an assessment of the clearance with statistically significant coefficients was developed.

ARTICLE HISTORY

Received : 25th Apr. 2022
 Revised : 04th Sept. 2023
 Accepted : 30th Nov. 2023
 Published : 20th Mar. 2024

KEYWORDS

Vibration
Suspension
EUSAMA
Wavelet decomposition
Parameter sensitivity
Diagnostic algorithm
Condition-based maintenance

1.0 INTRODUCTION

The procedure to evaluate the technical condition of a vehicle includes the evaluation of the condition of subcomponents and assemblies that are of key importance for the drivers and passengers safety, as well as environmental protection. Within the investigations carried out, the authors included the assessment of the suspension condition of the vehicle through the analysis of the damping efficiency in the European Shock Absorber Manufacturers (EUSAMA) test. This test involves measuring the static pressure on the EUSAMA platform. The diagnostic parameter is the EUSAMA index, which is the percentage ratio of the minimum pressure force on the platform (with the decreasing frequency of the shocks) to the static pressure force of the wheel on the said plate. This type of test focuses on the qualitative assessment of the level of disturbance in the suspension operation. The general condition of the suspension is also influenced by the rigidity of its components, vehicle load, tyre pressure, disturbances related to dry friction and pneumatic radial properties [1]–[4]. This condition is also influenced by the quality of the detachable connections, including the shock absorber mounting point to the body. Furthermore, as indicated in [5] the results of the EUSAMA test of vehicles fitted with a modern suspension may not reflect its actual condition. During the vehicle operation, shock absorber mountings develop a clearance that can have a negative impact on suspension conditions and traffic safety.

The authors of the article [6] from 2002 highlight the need for non-invasive tests to assess the condition of a vehicle's suspension system. Simultaneously, they introduce a model to identify its parameters using only non-invasive signals. The objective to minimise is the difference between the actual and predicted power spectrum of the output signal. This optimisation problem is tackled using the MRCD genetic algorithm. The authors also emphasise the need for faster diagnostic methods. Article [7] from 2023 focusses on detecting faults in the suspension system of road vehicles. An innovative methodology is presented that is capable of obtaining a full force-velocity characteristic of the shock absorber without the need for its disassembly. The appropriate tyre model plays a crucial role, allowing an accurate assessment of the shock absorber's performance. Using evolutionary algorithms for optimisation, the methodology has been validated through tests in an experimental vehicle, demonstrating its ability to detect subtle differences between shock absorbers.

The article [8] presents an analysis of a modified quarter-car model featuring a twin-tube hydraulic shock absorber with an added double-chamber cylinder. Unlike traditional dampers, this shock absorber's oil flow is regulated by the relative movement of an auxiliary piston and the pressure differences in adjacent chambers. A key feature is the non-linear spring element – the bumper – which safeguards the shock absorber from damage during large excitation amplitudes. The modified design alters the damping force characteristics, improving driving comfort at low amplitudes and high frequencies while increasing safety during resonance ranges. The study evaluates the system to various excitations, assessing the impact on driving comfort and safety. Numerical simulations, including spectral analyses, demonstrate the benefits of the modified shock absorber, particularly in reducing vibration amplitudes at high frequencies, thus improving driving comfort and safety, especially on well-maintained roads at high speeds.

The literature analysis concerning the assessment of a vehicle's technical condition, especially its suspension, reveals a diversity of approaches and research methods employed by various authors. The EUSAMA test, which focusses on

*CORRESPONDING AUTHOR | T. Nowakowski | ✉ tomasz.nowakowski@put.poznan.pl

measuring static pressure, serves as one of the tools to evaluate damping efficiency. However, its results may not accurately reflect the actual state of modern suspension systems. Several factors influence the overall condition of the suspension, including the rigidity of its components, vehicle load, and radial properties of tyres. The authors of various articles emphasise the need for non-standard tests and diagnostic methods. All studies underscore the importance of precise diagnostics and assessment of suspension conditions for road safety. Despite advances in this field, numerous aspects require further research. This particularly pertains to the assessment of clearance in shock absorber mounting points and the role the EUSAMA test might play in obtaining additional insight into the suspension's condition. The literature also indicates the need for further development of faster and more efficient diagnostic methods.

Building on the foundational understanding of the technical assessment, it is crucial to delve deeper into the practical aspects of shock absorber mounting. The mounting points, both upper and lower, play a key role in the overall performance and safety of the suspension system. At the upper point of mounting the shock absorber, the clearance can be compensated for with a nut. It is also easier to assess during diagnosis [9]. The lower shock absorber mounting point is not adjustable. Due to the specificity of this mounting, it is also impossible to quantitatively assess clearance. For this reason, only a qualitative assessment is carried out. Therefore, the authors propose to use the EUSAMA test to obtain additional feedback on suspension condition, which is understood as the clearance assessment of the shock absorber at the mounting point (Figure 1).

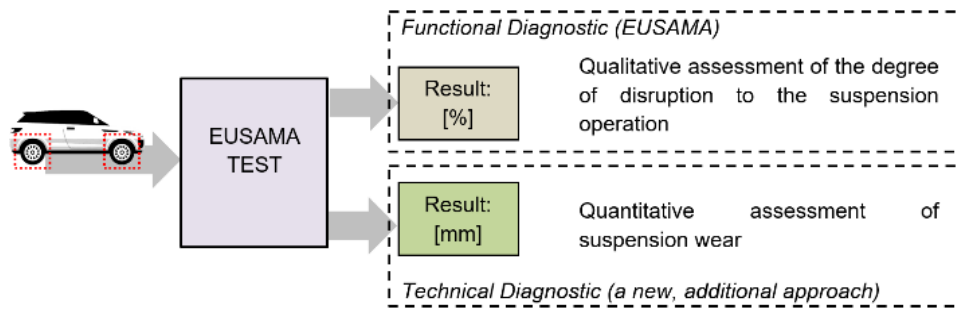


Figure 1. The tasks of functional and technical diagnostics in diagnosing the suspension condition of the vehicle suspension

For a quantitative assessment of the clearance at the lower shock absorber mounting point during EUSAMA suspension diagnostics, the authors propose to use vibration signals received and measured near the said mounting point. To estimate this clearance, a wavelet analysis of the vibration signals recorded through the vibration transducers located in the vicinity of the mounting can be applied. The assessment was preceded by an active experiment that simulated clearance in the mounting. This paper presents the course of the active experiment, the results of the measurements, and their wavelet decomposition, which allow for the estimation of the clearance at the lower mounting point of the shock absorber.

Figure 2. presents the schematics of the mathematical model that demonstrates the clearance problem based on the quarter-car model. This figure also presents the schematics of the mathematical model that describes the movement of the vehicle suspension quarter with suspension clearance (on the right) and without suspension clearance (on the left).

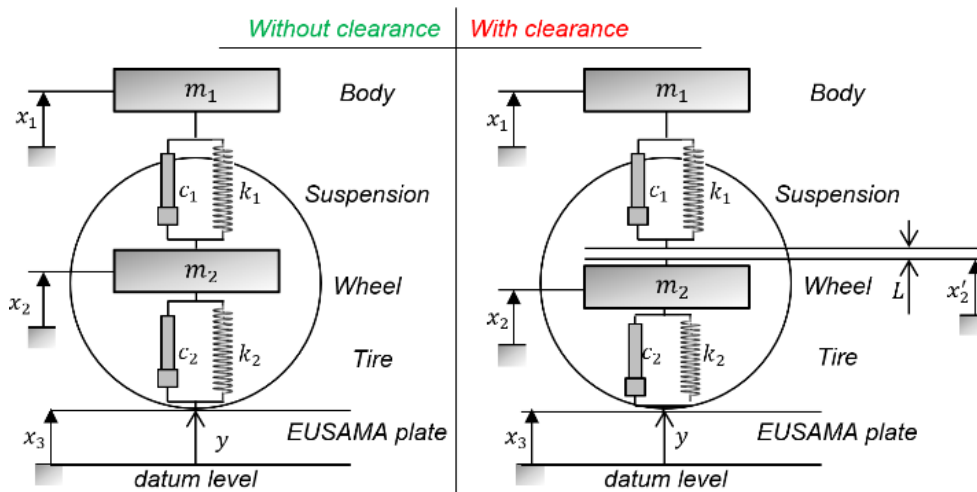


Figure 2. Quarter-car model illustrating aspects of clearance

Given the complexity of vehicular dynamics, the model presented offers a comprehensive approach to understanding the system's behaviour under varying conditions. The analysed model includes three cases: when $L = 0$, the motion of the system with two degrees of freedom can be described by the differential equation system (1):

$$\begin{cases} m_1\ddot{x}_1 + c_1(\dot{x}_1 - \dot{x}_2) + \\ + k_1(x_1 - x_2) = 0 \\ m_2\ddot{x}_2 + c_1(\dot{x}_2 - \dot{x}_1) + k_1(x_2 - x_1) \\ + c_2(\dot{x}_2 - \dot{x}_3) + k_2(x_2 - x_3) = 0 \end{cases} \quad (1)$$

when $L > 0$, the arrangement produces two systems, each with one degree of freedom. These systems are described by Equations (2) and (3).

$$M\ddot{x}_1 = Mg \quad (2)$$

$$m_2\ddot{x}_2 + c_2(\dot{x}_2 - \dot{x}_3) + k_2(x_2 - x_3) = 0 \quad (3)$$

The primary objective of the research delineated in this article is to meticulously detect and evaluate the clearance, using the vibration response to the excited force $F(t, L)$. Previous studies, such as those presented in [10], have elucidated the impact of vehicle operational conditions on its vertical dynamic response, predominantly validating the application of linear models for roads of acceptable quality. However, the evolution of vehicle suspension solutions and the increasing intricacies of modern designs underscore the potential necessity for the incorporation of non-linear models, as suggested in [5], [10].

Furthermore, it is paramount to consider the potential externalities and constraints that might influence the system's behaviour. Future research efforts could include the integration of advanced computational techniques and real-world testing to further refine and validate the proposed model. This would not only improve accuracy but also broaden its applicability across a broader spectrum of vehicle designs and road conditions.

2.0 RESEARCH METHODOLOGY

2.1 Assumptions

In the described diagnostic problem, the state-signal relation was determined based on the assumptions of an active experiment with a controlled change of object state characteristics $S(\theta)$ and a known, constant control vector $E(\theta)$. The basic diagnostic equation (4) has been shown below:

$$S(\theta) = \Phi[U(\theta), E(\theta), Z(\theta)] \quad (4)$$

Vectors representing state characteristics constitute the set of clearance values at the lower suspension mounting point of the rear right wheel defined by equation (5):

$$U(\theta) = [L_1 \ L_2 \ L_3 \ L_4 \ L_5 \ L_6 \ L_7] \quad (5)$$

Changes in suspension state characteristics were carried out using bolts of different diameters establishing defined clearance values, ie, a state without clearance ($L = 0$ mm) and clearance states $L = 2-7$ mm with clearance of 1 mm (Figure 3.). The view of the lower mounting point during the tests is shown in Figure 4..

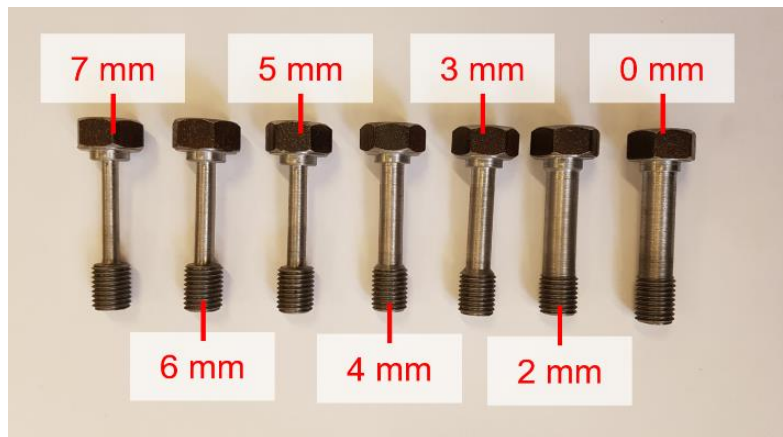


Figure 3. The set of screws of different diameters used for measurement during an active experiment



Figure 4. View of the suspension tested

The excitement of the vehicle suspension system was carried out using the FWT-1 type EUSAMA platform of the MAHA company (Figure 5.).



Figure 5. View of the EUSAMA test stand and car

The suspension system was increasingly placed in a vibration in the frequency range of 0.5 Hz to 15 Hz. Then, in the fading vibration, it passes through its resonance area. During the experiment, the authors ensured a constant control vector $E(\theta)$:

$$E(\theta) = [w_p \ t_t \ t_p \ s_t \ w_e] \quad (6)$$

The possible influence of the disturbances $Z(\theta)$ was minimized. Assuming $E(\theta)=const.$, $Z(\theta)=const.$ and $Z(\theta)=min.$ the following relation was obtained:

$$U(\theta) = S(\theta) \quad (7)$$

This equation signifies a pivotal understanding: to accurately evaluate the technical state of a given system, it is imperative to discern the parameter vector of signals produced by the said system. Furthermore, it suggests that the primary determinant that influences the measured signals is the variation in technical conditions. This insight underscores the importance of continuous monitoring and diagnostic evaluations, especially in dynamic systems such as vehicle suspensions, where even tiny changes can have profound implications on overall performance and safety.

2.2 Measurement points

The vibration transducer (accelerometer 4391 by Brüel & Kjaer) was installed at the lower point of the shock absorber mounting (Figure 6). Estimation of state using an acceleration sensor is commonly known. The examples are related to research by previous authors [9] or the estimation of the velocity of semi-active dampers in cars [11].



Figure 6. View of accelerometers location

The selection of the fitting method and location of the sensor resulted from the following:

- convergence of the directions of the excited vibration and the recorded one,
- the distance between the point of vibration generation and vibration reception,
- ease of fitting and access to the fitting point.

The reception, measurement and recording of the vibration signals received from the vibration sensor was carried out with the Brüel & Kjaer LAN-XI 3050 data acquisition module. In addition, the synchronous platform parametrizes with the vibration transducer as well as the parameters of the suspension system condition by measuring the adhesion of the wheel to the platform using the EUSAMA index.

2.3 Assumptions of the wavelet MRA analysis

To date, the experience of the authors in diagnostics of the technical condition of the upper mounting point of the shock absorber using the EUSAMA procedure has allowed the development of a vibration diagnostic parameter whose sensitivity to change of technical condition was 58% [9]. In the work on methods of diagnosing the lower mounting point of the shock absorber, the authors have adopted a novel approach based on wavelet multiresolution analysis (MRA). MRA stands out as a transformative analytical tool that offers the ability to decompose a signal into varying levels of resolution or components. This decomposition is not merely a mathematical exercise; each component encapsulates specific information and, when combined, they can faithfully reconstruct the original signal. This multi-layered decomposition facilitates a greater understanding of the signal, segregating data variability into components that are both physically significant and interpretable.

One of the salient features of MRA is its ability to provide information on the frequency components of the signal. As the resolution escalates, the data encapsulate information pertaining to higher frequency components, offering a granular view of the signal's behaviour. The MRA's methodology is underpinned by a filtering approach, specifically leveraging half-band filters. These filters play a pivotal role in bifurcating the signal into two distinct categories: low-frequency approximations (denoted as 'a') and high-frequency details (denoted as 'd'). This dichotomy, visually represented in Figure 7., provides a comprehensive overview of the signal characteristics, enabling a more informed diagnostic process. The authors' innovative approach, combining traditional diagnostic methods with advanced analytical tools like MRA, paves the way for future research and applications in vehicular diagnostics.

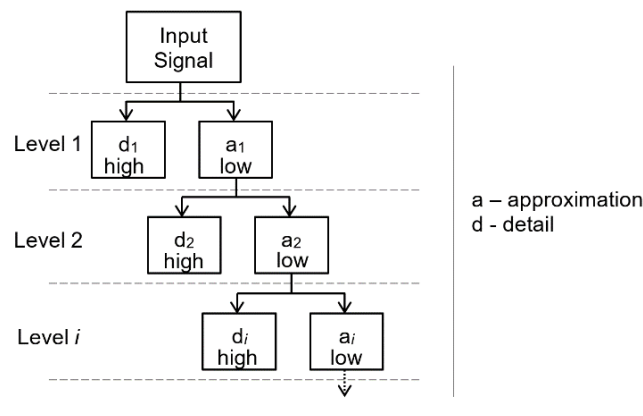


Figure 7. The tree of signal decomposition in MRA analysis

The discrete wavelet transform in MRA builds a tree of decomposition iteratively using the scaling and the wavelet function by a set of low-pass and high-pass filters. Discrete Wavelet Transform (DWT) is expressed as in the eqs. [12]:

$$a^j(n) = \sum_{i=0}^{L-1} l(i)a^{j-1}(2n - i), 0 \leq n \leq N_j \tag{8}$$

$$d^j(n) = \sum_{i=0}^{L-1} h(i)d^{j-1}(2n - i), 0 \leq n \leq N_j \tag{9}$$

The application of filters to the input signal of the frequency band $0-f$ containing N samples results in the reduction of the band by half $0-f/2$ and the obtaining of information on the approximate and detail. The Nyquist rule is applied, which prevents the loss of information. First, the filters allow for the entire frequency band (level 1) and then gradually narrow them at subsequent levels, allowing for subsequent low-pass output. In order to carry out MRA, orthogonal wavelets, i.e. Daubechies or Coiflets, are applied to successfully separate the low frequencies from the high frequencies of the signal. MRA allows for visualising the variability of the signal on different scales or frequency bands at the same time. The wavelet transforms (DWT) has led to great advances in many fields of science, whereas MRA analysis has already been used in many scientific applications.

The use of MRA facilitates the extraction of relevant vibration signal components when diagnosing faults in rotating machinery, such as bearings and gears. In different approaches, a mother wavelet was applied, most often the Daubechies family, such as Db4 [13], [14], Db5 [15], Db6 [16], [17], and Db8 [18]. The Db4 wavelet was also used in MRA analysis in the identification of structural damage [18], diagnostics of three-phase induction motors [19], or in the estimation of aerodynamic damping of a wind turbine [20]. The Db3 wavelet was used in the diagnosis of the health of a polymer electrolyte membrane fuel cell [21]. In [22] the applicability of the Db4 wavelet was confirmed in the MRA analysis carried out in the diagnosis of induction motors. In [23] a transmission line fault classification was presented, where 16 investigated to establish the superiority of the Db4 wavelet over other standard wavelets for accurate fault classification.

The MRA wavelet analysis was also successfully used to diagnose rail corrugation from the perspective of a rail vehicle (on-board) where the Debuchies wavelet was applied in a relatively high order Db7 [24]. The haar, Db2, and Db4 wavelets were used in the prediction technique by segregating a time series into linear and non-linear components [25]. MRA analysis is a useful tool for successful data de-noising that increases diagnostic efficiency [26]. MRA analysis is commonly used in medicine. An example of an application is an automatic cardiac arrhythmias diagnosis system based on ECG signals [27], or an intelligent approach to detect Covid-19 from chest radiographs [28]. The MRA wavelet is also commonly applied in analysis for image retrieval [29], or for adaptive colour multi-watermarking schemes for copyright protection [30].

3.0 RESULTS OF MEASUREMENTS AND THEIR WAVELET ANALYSIS

The results of the EUSAMA test were analysed as a function of the set clearance in the suspension mounting. The outcome is presented in Figure 8..

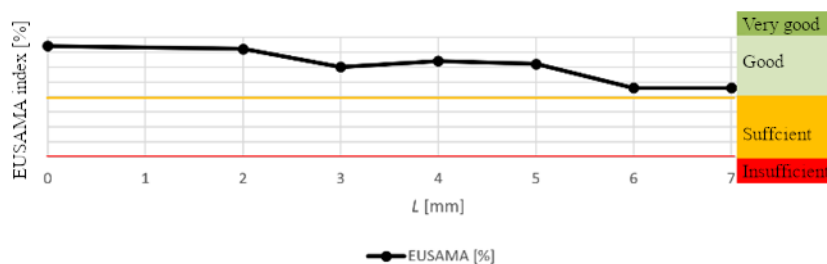


Figure 8. The EUSAMA index values as a function of suspension clearance

The data presented indicate that the EUSAMA index of the investigated object did not exceed the limit value of 20% resulting from the legislation [31] despite a clearance in the suspension mounting. Extreme clearance cases are greater than the limit value (by 3–5%). This deviation, although seemingly minor, has significant implications. For example, based on the data presented, a vehicle exhibiting a clearance of 7 mm would still be classified as roadworthy according to the EUSAMA test results. This underscores the potential limitations of relying solely on the EUSAMA index to determine vehicle roadworthiness, especially when clearances approach the upper limits of acceptability. The material collected during the experiment was time signals of vibration acceleration from the measurement points located on the platform (P) and suspension (S). The time tracings of the extreme cases of clearance and the intermediate cases of clearance are presented in Figure 9..

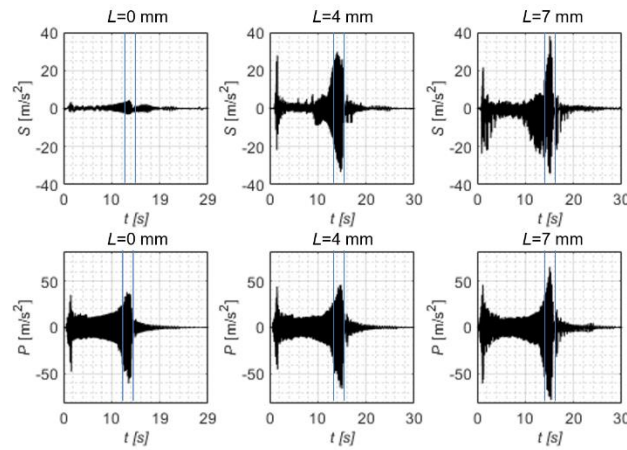


Figure 9. Time signals of the vibration acceleration from the suspension and the platform for selected clearance cases

On examination of Figure 9, it becomes evident that the time signals associated with the vibration acceleration of the vibration exhibit consistency. This can be attributed to the implementation of a well-structured and reproducible test procedure that ensures the reliability and repeatability of the results. However, a deeper dive into the data reveals pronounced disparities, particularly within the time window corresponding to the excitation of the resonance vibration of the suspension. This specific interval has been delineated with asymptotes on the tracings for improved clarity.

For a fully functional suspension system, the instantaneous absolute values hover around 4.5 m/s^2 . However, when clearances of 4 and 7 mm are introduced, these values escalate dramatically to 33.5 m/s^2 (reflecting an increase of +87%) and 38 m/s^2 (an increase of +88%), respectively. On the platform, the corresponding values for a good state suspension stand at 60.3 m/s^2 . When subjected to 4 mm and 7 mm clearances, these figures increase to 65.8 m/s^2 (+8%) and 78.0 m/s^2 (+23%), respectively. It should be noted that more dynamic fluctuations are observed at the suspension point. A higher dynamic of changes is observed at the point on the suspension, which is related to the occurrence of an additional vector of force generated at a distance L .

In the wavelet decomposition, a mother wavelet of the Daubechies family was applied. Such wavelets are orthogonal and allow the performance of multiresolution analysis, as they calculate both the scaling function and the wavelet. The Daubechies wavelets are the most appropriate functions for multi-resolution analyses because they have the properties of orthogonality and compact support. The authors decided to apply the Daubechies wavelet with 4 vanishing moments (Db4) that is successfully applied for quick and short periodic disturbances. Furthermore, the Db4 wavelet exhibits similarity to the phenomenon of clearance selection in suspension during the EUSAMA test, and the energy spectrum is concentrated around low frequencies.

Separation and inclusion of the ranges of components in the low-frequency analyses required decomposing the signals into 12 levels. The final approximation of the signal allowed for the range of the normalised frequency $0-0.000122$ cycles/sample, which, when considering the sampling frequency $f_s = 2^{12}$ Hz, corresponded to the range of approximately $0-8$ Hz. The details of the decomposition in the suspension example of the signal for $L = 4$ mm are presented in Table 1..

Table 1. Details of the *Sa* signal decomposition for the clearance value of $L = 7$ mm

Level	Frequencies (cycles/sample)	Relative energy
1	0.25 – 0.5	0.35%
2	0.121 – 0.259	0.18%
3	0.0603 – 0.129	0.09%
4	0.0302 – 0.0646	0.05%
5	0.0151 – 0.0323	0.04%
6	0.00754 – 0.0162	0.09%
7	0.00377 – 0.00808	0.18%
8	0.00188 – 0.00404	0.72%
9	0.000942 – 0.00202	0.91%
10	0.000471 – 0.00101	0.97%
11	0.000236 – 0.000505	7.23%
12	0.000118 – 0.000252	45.72%
approx.	0 – 0.000122	43.47%

In the detailed breakdown of the signal's energy distribution across various levels, a distinct pattern emerges that offers insights into the signal's composition and its inherent characteristics. Specifically, the initial levels, which range from 1 to 10, predominantly encapsulate the details of the signal. These details collectively contribute a minimal portion to the overall energy, with their relative energy not exceeding the 1% threshold. This suggests that, while these levels capture aspects of the signal, their cumulative impact on the signal's overall energy profile is relatively subdued. Transitioning to Level 11, there is a noticeable uptick in the energy contribution. This level alone represents 7.2% of the total energy, marking a significant increase compared to the preceding levels. Such a jump indicates that the components or features represented at this level play a more substantial role in shaping the signal's overall characteristics.

The final level contains a dominant 45.7% of the signal's energy. This substantial proportion underscores the critical importance of this level in defining the signal's overarching profile and dynamics. Furthermore, when considering the approximation of the signal, it is observed that it has a relative energy of 43.5%. This approximation essentially captures the core essence of the signal, and its energy contribution being close to that of the last level suggests that it effectively represents the primary components and patterns inherent in the signal.

In essence, this breakdown elucidates the hierarchical structure of the signal energy distribution, highlighting the varying importance of different levels and the overarching importance of the signal's approximation in capturing its primary characteristics. The decomposition of the signal at the suspension measurement points for $L=4$ mm is shown in Figure 10..

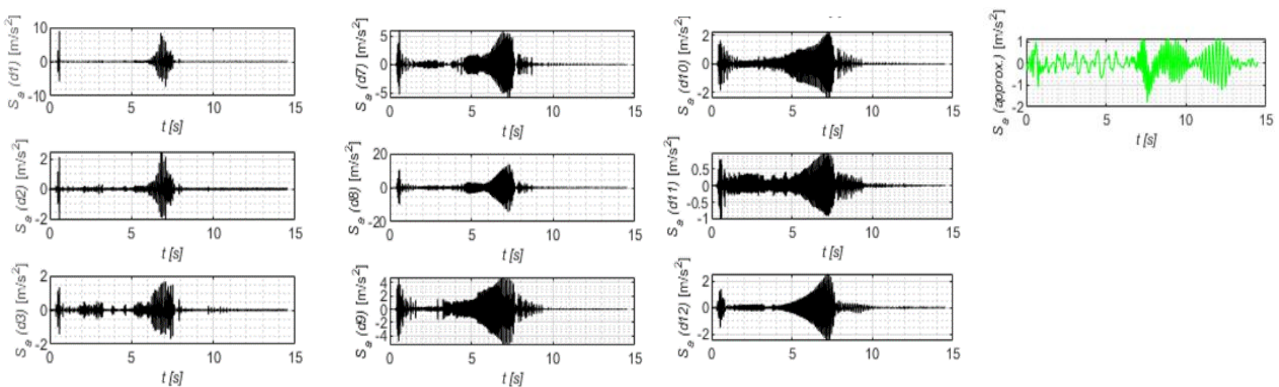


Figure 10. Decomposition of the suspension signal for the clearance value of $L=4$ mm

In the presented study, the authors used the signal approximation obtained from wavelet decomposition. This was achieved by deducing high-frequency details from the primary signal, thereby refining the data for a more precise interpretation. The original time signals comparison and the approximate decomposition for extreme cases of the suspension condition are shown in Figure 11..

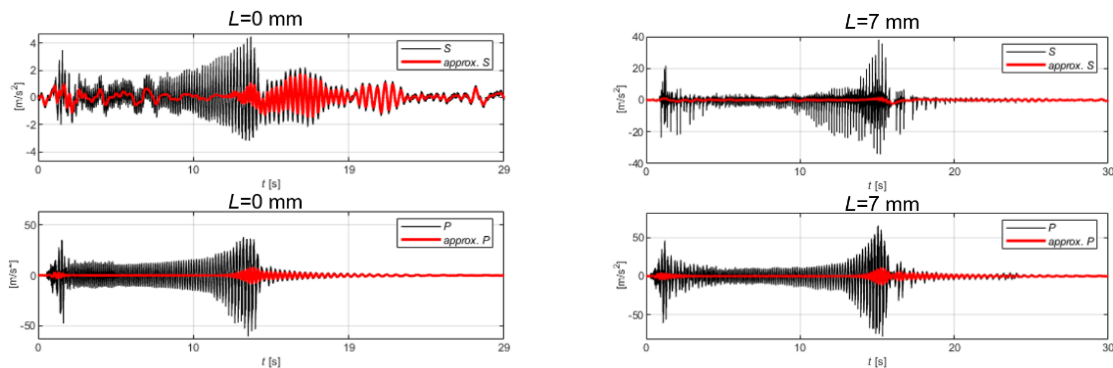


Figure 11. Comparison of the original time signals with the approximated wavelet decomposition for the condition of fully operative suspension and the clearance value of $L = 7$ mm

It was assumed that the observation of dynamic phenomena in the vibration acceleration signal should comprise the range of the greatest shocks of the platform prior to the occurrence of suspension resonance. Analyses performed during the appearance of suspension resonance are not conclusive in terms of the interpretation of the results as a function of the set clearance due to the lack of stability of the system. Moreover, the proposed approach enables the minimisation of the disturbances and assurance of constant control conditions in the experiment. The detection of increased interactions was performed based on the observation of the measure proportional to the power of the signal in the form of a floating efficient value of the approximated signal of the platform, calculated as in the equation:

$$S_{RMS(approx.)}(t) = \sqrt{\frac{1}{T_0} \int_{t-T}^t x^2 dx} \tag{10}$$

The number of samples in the signal window T was $N=2^{12}$ and the sampling time was $dr=0.0625$ s. An example of the detection of increased dynamic interactions is shown in Figure 12..

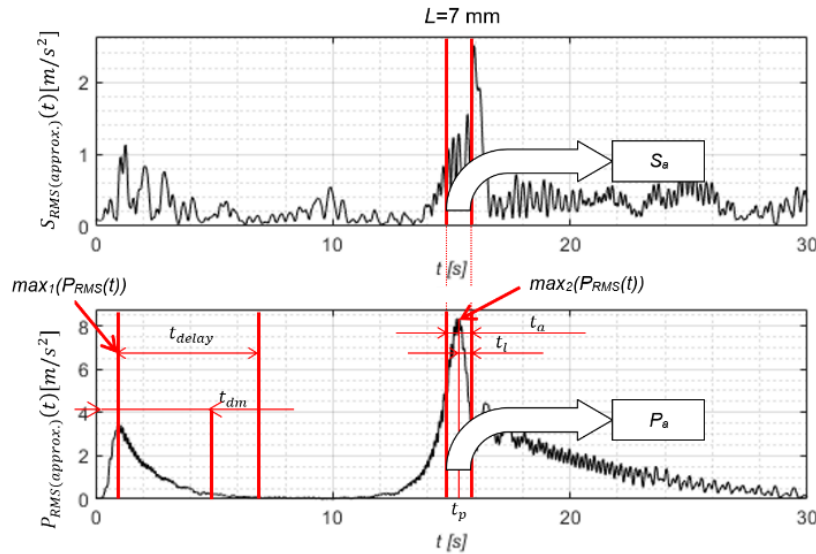


Figure 12. Example of the detection of increased dynamic interactions based on $S_{RMS(t)}$ for a configuration with the clearance value of 7 mm

The detection of the signal was related to the identification of the maximum value $max_1(P_{RMS}(t))$ at time $tdm = 3$ s related to the start of the EUSAMA test. Subsequently, the detection of the maximum value $max_2(P_{RMS}(t))$ occurred when the test initiation stopped (delay $t_{delay}=6$ s) covering the range of the highest shocks on the platform. In the next step, a time selection of the signals was performed for further analyses. It was based on cutting a fragment of the signal $t_a=1$ s referring to t_p , that is, the occurrence of the maximum value $max_2(P_{RMS}(t))$. The fragment t_a was characterized by the relation $t_p = \frac{t_a}{2}$. Based on times $t_p \pm t_l$, signals P_a and S_a were selected.

For the selected fragments P_a and S_a , a parameterisation of the dynamic phenomena was carried out by calculating the quantitative measures in the form of a crest factor (CF), kurtosis (K), skewness (SK), maximum (MAX) and minimum (MIN) as in equations (11-13) below:

$$CF = \frac{x_{MAX}}{x_{RMS}} \tag{11}$$

$$K = \frac{N(N+1)}{(N+1)(N+2)(N+3)} \sum_{i=1}^N \left(\frac{x_i - \bar{x}}{\sigma}\right)^4 - \frac{3(N+1)}{(N-2)(N-3)} \tag{12}$$

$$SK = \sum_{i=1}^N \frac{(x_i - \bar{x})^3 / N}{\sigma^3} \tag{13}$$

The authors then performed a parameter normalisation to obtain dimensionless parameters to enable comparison of their trends. Normalisation was carried out according to the first observation according to Equation (14):

$$X'_i = \frac{x_i}{x_1} \tag{14}$$

Upon normalisation, the authors performed a selection of the parameters that met the condition of conclusiveness. Out of the calculated measures, only one parameter $S_{a(MAX)}$ satisfied this condition. The EUSAMA test results in Figure 13 displayed this parameter.

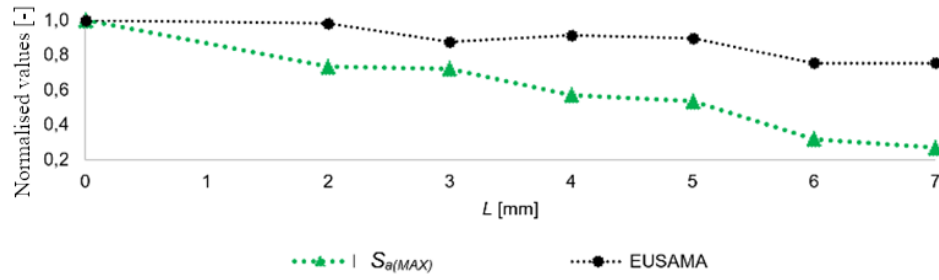


Figure 13. Normalised values of the EUSAMA index and parameter $S_{a(MAX)}$ as a function of the clearance of the set clearance

Next, the sensitivity of the parameters was calculated, defined as in Equation (15):

$$WR = \sum_{i=1}^7 (X'_{i+1} - X'_i) \cdot 100\% \tag{15}$$

The parameter $S_{a(MAX)}$ was characterised by a sensitivity at the level of 73% and the EUSAMA index was found to be at 25%. The EUSAMA index was not conclusive – an extreme occurred at $L=3$ mm. The results obtained confirm the applicability of the method and the usefulness of the parameter $S_{a(MAX)}$ in assessing suspension clearance.

4.0 MODELLING OF THE DIAGNOSTIC PARAMETER

For the developed parameter $S_{a(MAX)}$, the authors created models for suspension assessment clearance. A total of five different models were examined, including polynomial, gauss, and exponential models. Figure 14. presents the above-mentioned models.

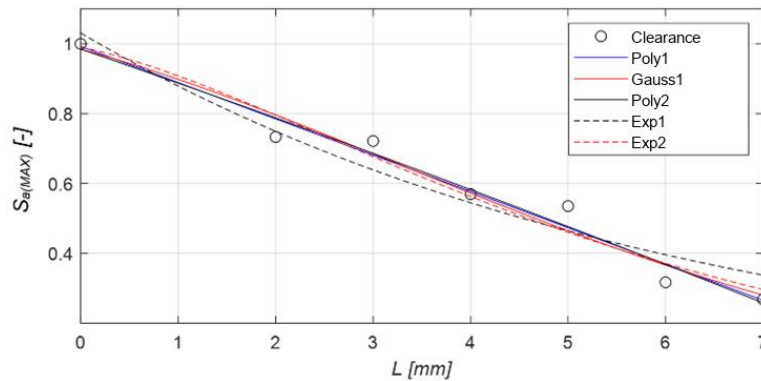


Figure 14. Models of evaluation of suspension clearance based on the parameter $S_{a(MAX)}$

The equations (16-20) of the models are shown below:

$$S_{a(MAX)poly1} = -0.10392L + 0.99297 \tag{16}$$

$$S_{a(MAX)gauss1} = 1.0890e \left(- \left(\frac{(L - 2.6254)}{8.2635} \right)^2 \right) \tag{17}$$

$$S_{a(MAX)poly2} = -0.0010764x^2 - 0.096294L + +0.98494 \tag{18}$$

$$S_{a(MAX)exp1} = 1.0312 \exp (-0.15948L) \tag{19}$$

$$S_{a(MAX)exp2} = 6811.8 \exp(-0.32275L) - 6810.8 \exp (-0.32279L) \tag{20}$$

Regression models must be statistically validated. Validation of the models was carried out by determining a series of statistical data. First, the authors determined the fitness level of the models using the actual data. For this reason, a coefficient of determination R^2 was obtained. In order to determine the significance of individual regression coefficients, the authors proposed hypotheses, described by equations (21-22) below:

$$H_0: \beta_j = 0 \tag{21}$$

$$H_1: \beta_j \neq 0 \tag{22}$$

Rejecting H_0 signifies having statistical grounds to state that there exists a correlation between the dependent variable and at least one independent variable. To test hypotheses related to the determination of the statistical significance of the individual regression coefficients, the authors used a distribution of t-students. In the investigations, the authors adopted statistical significance at the level of $\alpha=0.05$. The results of the statistical analysis for the models can be viewed in Table 2 and Table 3..

Table 2. Results of the statistical analysis of the polynomial and Gaussian models of the parameter $S_{a(approx. MAX)}$

	poly1		gauss1		poly2	
RMSE	0.047		0.057		0.052	
R^2	0.972		0.966		0.972	
Coeff.	Est.	p	Est.	p	Est.	p
1	-0.1039	4.67E-05	1.0890	9.00E-03	-0.0010764	8.03E-01
2	0.9930	1.08E-06	-2.6254	4.30E-01	-0.096294	3.21E-02
3	–	–	8.2635	2.21E-02	0.98494	3.75E-05

Table 3. Results of the statistical analysis of the exponential models of the parameter $S_{a(approx. MAX)}$

	expl		exp2	
RMSE	0.070		0.062	
R^2	0.936		0.960	
Coeff.	Est.	p	Est.	p
1	1.0312	1.52E-05	6811.8	2.56E-21
2	-0.15948	4.49E-04	-0.32275	7.36E-03
3	–	–	-6810.8	2.56E-21
4	–	–	-0.32279	7.37E-03

When analysing the results, the authors have observed that the gauss1 and poly2 models, described with equations (17) and (18) respectively, contained statistically insignificant coefficients, which is why these models were eliminated from further investigations. The authors assumed that they would select a regression model, for which the coefficient of determination is equal to or greater than 0.90, which has the lowest RMSE value of all models and its model coefficients are statistically significant. Based on these criteria, the authors selected the poly1 model as the best way to assess suspension clearance based on the diagnostic parameter. The coefficients obtained indicate that this model can accurately forecast the data.

5.0 VALIDATION OF THE DIAGNOSTIC PARAMETER

In the next part of the work, the obtained model was validated by taking measurements for a larger group of clearances. The validation involved measurements with values $L_V=0.5-7$ mm with a step 0.5 mm, creating a clearance validation vector defined by equation (23):

$$U_V(\theta) = [L_{V1}, L_{V15}] \tag{23}$$

Measurements were made while maintaining the original test methodology and the control conditions in the experiment presented in equation (3). The results of the measurement validation are presented in Figure 15.

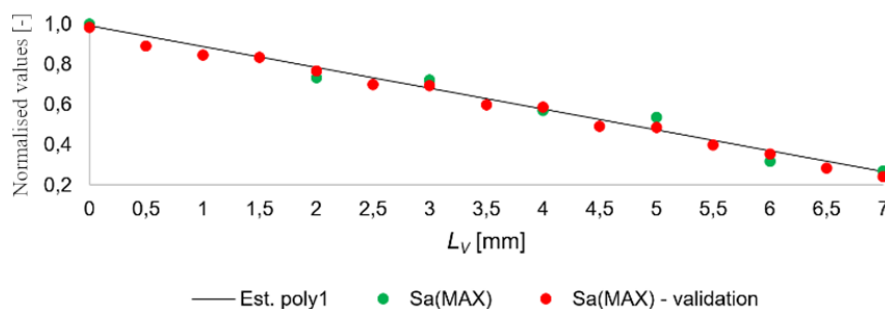


Figure 15. Normalised values of the parameter $S_{a(MAX)}$ as a function of the set validated clearance L_V

For the data obtained, the prediction error (PE) was calculated according to the following equation:

$$PE = \frac{|x_{a,i} - x_{m,i}|}{x_{m,i,j}} \tag{24}$$

The statistics of the prediction error PE are shown in Figure 16.

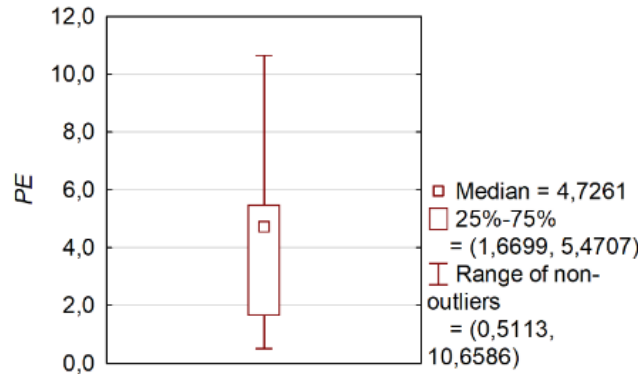


Figure 16. Overview of the prediction error (PE) from validation measurements

The comprehensive validation process yielded insightful findings regarding the accuracy and reliability of the proposed model. Specifically, within the 25–75% range, which can be considered the interquartile range and often represents the central tendency of a dataset, the model showcased a prediction error of up to 6%. This suggests that for most of the data points within this central range, the model predictions deviated from the actual values by a relatively small margin, underscoring its efficacy. However, when the scope was extended to encompass all measurements, the prediction error increased, reaching up to 11%. Although this is a larger deviation compared to the interquartile range, it is essential to consider the inherent variability and potential outliers present in a complete data set, which can influence the overall error rate. In particular, the median prediction error, which represents the middle value when the errors are arranged in ascending order, was found to be approximately 5%. This median value further emphasises the model's overall robustness and reliability of the model, since half of the prediction errors were below this threshold. In summary, the validation results underscore the model's potential as a reliable predictive tool, and its performance is exceptionally well within the central data range.

6.0 DIAGNOSTIC ALGORITHM

The suspension clearance presented in Figure 16., has four crucial stages. The first stage involves recording the time tracings from the platform and suspension during the EUSAMA test. In the second stage, an MRA wavelet analysis is performed in order to obtain the approximation signals from the 12 levels of signal distribution. In the third stage, the input signals are prepared for calculating the diagnostic parameter which is related to the final stage. In the final clearance stage, the assessment is performed and the excess of the set boundary value (S_g) is verified. This value should be in accordance with the legislation related to the vehicle road worthiness (or non-roadworthiness) based on the suspension clearance.

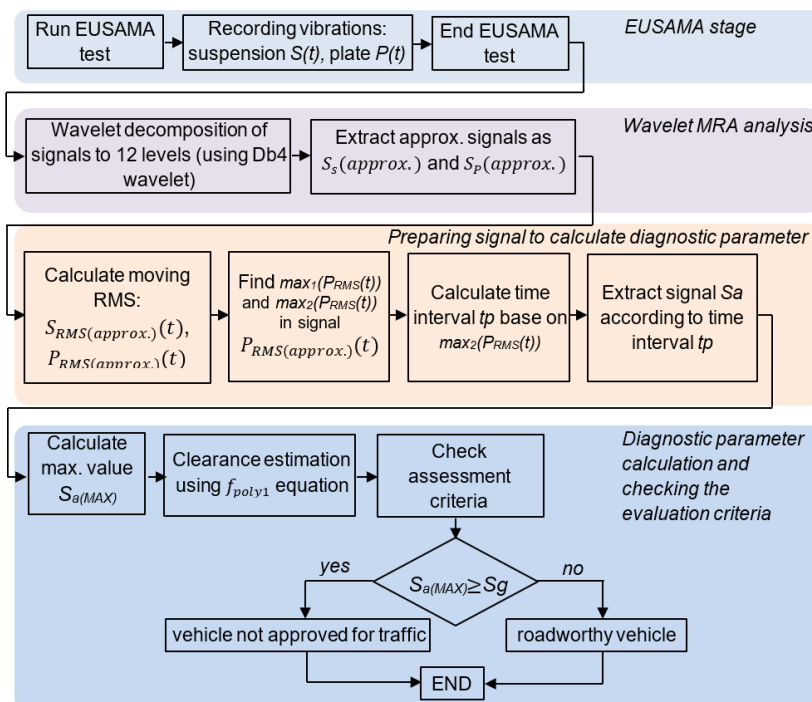


Figure 16. Algorithm to assess suspension clearance

The authors propose a criterion for roadworthiness, which is $Sg \geq 0.89$. This value corresponds to the suspension clearance value of $L=1$ mm. A clearance value of $L=1$ mm might represent a balance between performance and wear. While larger clearances could lead to decreased performance or increased wear and tear, smaller clearances may not offer significant performance benefits to justify the potential risks or costs. By applying a specific criterion, it becomes easier to predict when maintenance or replacements may be necessary. If the vehicle's system starts approaching the $Sg \geq 0.89$ threshold, it could be an indicator that maintenance is due soon.

7.0 DISCUSSIONS

The field of vehicle suspension diagnostics is complex and requires a balance between precision and practical applicability. The research presented in this work underscores the potential of technical diagnostics to address both of these facets. The $S_{a(RMS)}$ diagnostic parameter, with its increased sensitivity, emerges as a promising tool in this endeavour. Wavelet multiresolution analysis (MRA) plays a pivotal role in providing a signal that transmits invaluable diagnostic information. This aspect is crucial for a holistic understanding of the implications of the research.

The noninvasive nature of the proposed methodology aligns with the broader industry trend. This is a significant point of discussion, as the automotive industry is increasingly leaning toward methodologies that minimise intrusive diagnostic procedures. Implementing such an approach not only ensures the vehicle's integrity but also streamlines the diagnostic process, making it more efficient and user-friendly. For that reason, the addition of wireless vibration transducers to the existing EUSAMA test could provide faster diagnostic information. Such wireless technology would enhance the data acquisition process, making it more efficient.

The presented method has been validated for a vehicle with an approximate weight of one ton. Future research should extend this validation to vehicles of greater mass to ensure the universality of the method. Furthermore, the method has not been validated on any other EUSAMA test platform (other than FWT-1 by MAHA). Given that the procedure is regulated by law, similar results are expected on different platforms. Another avenue of exploration is the simulation of damage to the lower suspension mounting of the vehicle. The current study employed a specific approach, but alternative simulation methods might provide different insights. The validation process, with its prediction error margin confined to 10%, suggests room for improvement. Future research efforts could focus on harnessing advanced computational techniques or machine learning algorithms to further refine this model, enhancing its precision and reliability.

Looking ahead, it would be prudent to develop predictive models of damage. Such models, when combined with the EUSAMA test equipped with transducers, could help determine the estimated lifespan of the suspension, taking into account the average annual mileage of the vehicle in question.

8.0 CONCLUSIONS

In rapidly evolving modern engineering, the continuous refinement and enhancement of existing methodologies is very important. The research presented in this work exemplifies this philosophy, focussing on the intricate diagnostics of road vehicles. The findings underscore the potential of technical diagnostics not only to assess the overarching technical condition but also to pinpoint specific wear indicators, such as clearance of the lower mounting point of the wheel suspension. By using the EUSAMA test, the proposed approach facilitates the acquisition of key operational data without significant modifications to conventional technical diagnostic procedures for road vehicles. The diagnostic parameter $S_{a(RMS)}$ introduced in this study stands out due to its increased sensitivity, registering a 48% higher response to variations in suspension condition compared to the conventional EUSAMA index. The introduction of the $S_{a(RMS)}$ diagnostic parameter, with its increased sensitivity, offers a new perspective on suspension diagnostics. Furthermore, wavelet multiresolution analysis (MRA) provides a signal that carries invaluable diagnostic information, which can ultimately be used in diagnostics.

Additionally, the model designed for clearance assessment demonstrated data supported by statistically significant coefficients providing practical applicability. The validation process further corroborated the efficacy of the model, showcasing a prediction error margin confined to 10%. Future research could investigate strategies to further narrow this margin, enhancing the model's precision. Furthermore, the non-invasive nature of the proposed methodology aligns with the broader industry trend of minimising intrusive diagnostic procedures, thereby ensuring that integrity remains uncompromised during assessments. In summary, while the research presented marks a significant step forward in the field of vehicle suspension diagnostics, it also sets the stage for future explorations, innovations, and refinements in this domain.

9.0 ACKNOWLEDGEMENT

All presented work is partially funded by the Statutory Activities Fund of the Institute of Transport, Poznan University of Technology (PL) 0416/SBAD/0005.

10.0 REFERENCES

- [1] P. Zdanowicz, "Assessment problems during the shock-absorbers condition test on EUSAMA stand (in Polish)," *Logistyka*, vol. 4 on CD, 2010.
- [2] J. Kupiec and G. Ślaski, "Mistakes in evaluating the damping ability of shock absorbers in testing with use the EUSAMA method (in Polish)," *Diagnostyka '30*, vol. 30, no. T.1, pp. 301–304, 2004.
- [3] M. Toma, C. Andreescu, and C. Stan, "Influence of tire inflation pressure on the results of diagnosing brakes and suspension," *Procedia Manufacturing*, vol. 22, pp. 121–128, 2018.
- [4] R. Jurecki, M. Kiewicz, and T. Wdowski, "Testing the influence of carload and pressure in tyres on the value of damping of shock absorbers specified with the use of the Eusama method," *Diagnostyka*, vol. 15, no. 3, 2014.
- [5] M. Klapka and I. Mazu, "Twilight of the EUSAMA diagnostic methodology," *Meccanica*, vol. 52, pp. 2023–2034, 2017.
- [6] A. Herreros, E. Baeyens, J. R. Perán, and A. Melgar, "Parameter identification of a car suspension system using non-intrusive signals," *IFAC Proceedings Volumes*, vol. 15, no. 1, pp. 427–432, 2002.
- [7] E. Carabias, J. A. Cabrera, J. J. Castillo, J. Pérez, and M. Alcázar, "Non-intrusive determination of shock absorber characteristic curves by means of evolutionary algorithms," *Mechanical Systems and Signal Processing*, vol. 182, p. 109583, 2023.
- [8] J. Łuczko and U. Ferdek, "Non-linear analysis of a quarter-car model with stroke-dependent twin-tube shock absorber," *Mechanical Systems and Signal Processing*, vol. 115, pp. 450–468, 2019.
- [9] G. M. Szymański, M. Jóska, F. Tomaszewski, and R. Filipiak, "Application of time-frequency analysis to the evaluation of the condition of car suspension," *Mechanical Systems and Signal Processing*, vol. 58, pp. 298–307, 2015.
- [10] Z. Klockiewicz, G. Ślaski, and M. Spadło, "The influence of the conditions of use and the type of model used on the vertical dynamic responses of a car suspension," *Archives of Automotive Engineering*, vol. 85, no. 3, pp. 57–82, 2019.
- [11] D. Lee, S. W. Jin, E. Rhee, and C. Lee, "Practical damper velocity estimation for semi-active suspension control," *International Journal of Automotive Technology*, vol. 22, no. 2, pp. 499–506, 2021.
- [12] S. G. Mallat, "A theory for multiresolution signal decomposition: the wavelet representation," *IEEE Transactions on Pattern Analysis and Machine Intelligence*, vol. 11, no. 7, pp. 674–693, 1989.
- [13] L. Liu, X. Song, K. Chen, B. Hou, X. Chai, and H. Ning, "An enhanced encoder – decoder framework for bearing remaining useful life," *Measurement*, vol. 170, p. 108753, 2021.
- [14] R. Brancati, E. Rocca, and S. Savino, "A gear rattle metric based on the wavelet multi-resolution analysis: Experimental investigation," *Mechanical Systems and Signal Processing*, vol. 50–51, pp. 161–173, 2015.
- [15] I. Moumene and N. Ouelaa, "Application of the wavelets multiresolution analysis and the high-frequency resonance technique for gears and bearings faults diagnosis," *International Journal of Advanced Manufacturing Technology*, vol. 83, no. 5–8, pp. 1315–1339, 2016.
- [16] C. Castejón, O. Lara, and J. C. García-Prada, "Automated diagnosis of rolling bearings using MRA and neural networks," *Mechanical Systems and Signal Processing*, vol. 24, no. 1, pp. 289–299, 2010.
- [17] J. Sanz, R. Perera, and C. Huerta, "Fault diagnosis of rotating machinery based on auto-associative neural networks and wavelet transforms," *Journal of Sound and Vibration*, vol. 302, pp. 981–999, 2007.
- [18] D. Li *et al.*, "A multiscale reconstructed attractors-based method for identification of structural damage under impact excitations," *Journal of Sound and Vibration*, vol. 495, p. 115925, 2021.
- [19] S. A. Saleh, M. Abdesh Khan, and M. A. Rahman, "Application of a wavelet-based MRA for diagnosing disturbances in a three-phase induction motor," *SDEMPED 2005 - International Symposium on Diagnostics of Electric Machines, Power Electronics, and Drives*, 2005.
- [20] B. Chen, B. Basu, X. Hua, *et al.*, "Online DWT algorithm for identification of aerodynamic damping in wind turbines," *Mechanical Systems and Signal Processing*, vol. 152, p. 107437, 2021.
- [21] J. Kim and Y. Tak, "Implementation of discrete wavelet transform-based discrimination and state-of-health diagnosis for a polymer electrolyte membrane fuel cell," *International Journal of Hydrogen Energy*, vol. 39, no. 20, pp. 10664–10682, 2014.
- [22] B. A. S. Houda and A. G. Mediha, "Multiresolution analysis based effective diagnosis of induction motors," *American Journal of Applied Sciences*, vol. 9, no. 5, pp. 624–632, 2012.
- [23] M. J. Reddy and D. K. Mohanta, "A DSP based frequency domain approach for classification of transmission line faults," *Digital Signal Processing: A Review Journal*, vol. 18, no. 5, pp. 751–761, 2008.
- [24] T. Kojima, H. Tsunashima, and A. Matsumoto, "Fault detection of railway track by multi-resolution analysis," *WIT Transactions on The Built Environment*, vol. 88, pp. 955–964, 2006.
- [25] I. Khandelwal, R. Adhikari, and G. Verma, "Time series forecasting using hybrid arima and ann models based on DWT Decomposition," *Procedia Computer Science*, vol. 48, no. C, pp. 173–179, 2015.
- [26] L. Jedliński, "Multi-channel registered data denoising using wavelet transform," *Eksploracja i Niezawodność – Maintenance and Reliability*, vol. 14, no. 2, pp. 145–149, 2012.
- [27] N. Sinha and A. Das, "Automatic diagnosis of cardiac arrhythmias based on three stage feature fusion and classification model using DWT," *Biomedical Signal Processing and Control*, vol. 62, p. 102066, 2020.
- [28] R. Mostafiz, M. S. Uddin, N. A. Alam, M. Mahfuz Reza, and M. M. Rahman, "Covid-19 detection in chest X-ray through random forest classifier using a hybridization of deep CNN and DWT optimized features," *Journal of King Saud University Computer and Information Sciences*, vol. 34, no. 6, part B, pp. 3226–3235, 2021.

- [29] N. S. T. Sai, R. Patil, S. Sangle, and B. Nemade, "Truncated DCT and Decomposed DWT SVD Features for Image Retrieval," *Procedia Computer Science*, vol. 79, pp. 579–588, 2016.
- [30] Y. Shen, C. Tang, M. Xu, M. Chen, and Z. Lei, "A DWT-SVD based adaptive colour multi-watermarking scheme for copyright protection using AMEF and PSO-GWO," *Expert Systems with Applications*, vol. 168, p. 114414, 2021.
- [31] *Regulation of the Polish Minister of Transport, Construction and Maritime Economy of 26 June 2012 on the scope and method of carrying out technical tests of vehicles and templates of documents used in these tests, Journal of Laws of 2012, Item 996. 2012.*